NACA

RESEARCH MEMORANDUM

AERODYNAMIC CHARACTERISTICS AT TRANSONIC SPEEDS OF A 60° DELTA WING EQUIPPED WITH A TRIANGULAR PLAN-FORM CONTROL HAVING A SKEWED HINGE AXIS AND AN OVERHANG BALANCE

TRANSONIC-BUMP METHOD

By Harleth G. Wiley

Langley Aeronautical Laboratory
Langley Field, Va.

NATIONAL ADVISORY COMMITTEE
FOR AERONAUTICS

WASHINGTON
February 6, 1951

NATIONAL ADVISORY COMMITTEE FOR AERONAUTICS

RESEARCH MEMORANDUM

AERODYNAMIC CHARACTERISTICS AT TRANSONIC SPEEDS OF A 60° DELTA WING EQUIPPED WITH A TRIANGULAR PLAN-FORM CONTROL HAVING A SKEWED HINGE AXIS AND AN OVERHANG BALANCE

TRANSONIC-BUMP METHOD

By Harleth G. Wiley

SUMMARY

An investigation to determine the aerodynamic characteristics of a semispan delta wing equipped with an aerodynamically balanced triangular control mounted on a skewed hinge axis was made in the Langley high-speed 7- by 10-foot tunnel by means of the transonic-bump method. The wing had 60° of sweepback at the leading edge, an aspect ratio of 2.31, a taper ratio of 0, and an NACA 65-006 airfoil parallel to the free air stream. Lift, drag, pitching-moment, rolling-moment, and hinge-moment data are presented for a range of angle of attack and control deflection through a Mach number range of 0.6 to 1.18. The mean Reynolds numbers at which the tests were conducted varied from 1,100,000 to 1,500,000.

The data indicate that the balanced control was effective in producing changes in lift, pitching moment, and rolling moment at all Mach numbers investigated. The control was overbalanced in the low ranges of control deflection and angle of attack and was more sensitive to changes in Mach number than was an unbalanced triangular control of generally similar plan form.

INTRODUCTION

Because of the urgent need for aerodynamic data in the transonic speed range, an integrated program of transonic research has been initiated by the National Advisory Committee for Aeronautics. As an extension of the transonic research program, a series of delta-shaped

wings with 60° of sweepback at the leading edge and with various control-surface configurations are being investigated by the transonic-bump method in the Langley high-speed 7- by 10-foot tunnel.

Presented in this paper are the results of an investigation of a semispan model of a delta wing with 60° sweepback at the leading edge which was equipped with a large triangular control having an overhang balance mounted on a skewed hinge axis. The purpose of this investigation was to determine the aerodynamic characteristics of a delta wing with a control which was designed to provide aerodynamic balance at zero control deflection based on the span load distribution of reference 1.

COEFFICIENTS AND SYMBOLS

C_L lift coefficient $\left(\frac{\text{Twice lift of semispan model}}{qS}\right)$

ΔC_L incremental lift coefficient contributed by deflection of control at $\alpha = 0°$, $\left(C_L - C_{L_{\delta=0°}}\right)$

C_D drag coefficient $\left(\frac{\text{Twice drag of semispan model}}{qS}\right)$

C_l rolling-moment coefficient at plane of symmetry $\left(\frac{\text{Rolling moment of semispan model}}{qSb}\right)$

C_m pitching-moment coefficient referred to $0.25\bar{c}$ $\left(\frac{\text{Twice pitching moment of semispan model}}{qS\bar{c}}\right)$

C_h control hinge-moment coefficient about hinge axis $\left(\frac{\text{Hinge moment}}{2M_1 q}\right)$

q effective dynamic pressure over span of model, pounds per square foot $\left(\frac{1}{2}\rho V^2\right)$

S twice wing area of semispan model, 0.144 square foot

b twice span of semispan model, 0.578 foot

$\bar{c}$ mean aerodynamic chord of wing $\left(\frac{2}{S}\int_0^{b/2} c^2\,dy\right)$, 0.333 foot

c local wing chord, feet

y spanwise distance from plane of symmetry

M_l area moment of control surface aft of hinge axis, measured about hinge axis, 0.00113 foot cubed

ρ mass density of air, slugs per cubic foot

V average free-stream air velocity, feet per second

M effective Mach number over span of model

M_a average chordwise Mach number

M_l local Mach number

R Reynolds number of wing based on $\bar{c}$

α angle of attack, degrees

δ control deflection relative to wing-chord plane, measured perpendicular to control hinge axis (positive when trailing edge is down), degrees

$$C_{L_\delta} = \left(\partial C_L/\partial\delta\right)_\alpha$$
$$C_{l_\delta} = \left(\partial C_l/\partial\delta\right)_\alpha$$
$$C_{m_\delta} = \left(\partial C_m/\partial\delta\right)_\alpha$$
$$C_{h_\delta} = \left(\partial C_h/\partial\delta\right)_\alpha$$

The subscript α indicates that the angle of attack was held constant at $\alpha = 0^\circ$.

$$C_{h_\alpha} = \left(\partial C_h/\partial\alpha\right)_\delta$$

The subscript δ indicates that the control deflection was held constant at $\delta = 0^\circ$.

MODEL AND APPARATUS

The semispan wing had 60° of sweepback at the leading edge, 0° sweep at the trailing edge, with a taper ratio of 0, an aspect ratio of 2.31, and an NACA 65-006 airfoil section parallel to the free air stream. A sketch of the model as mounted on the bump in the tunnel is presented in figure 1. The wing was made of a bismuth and tin alloy bonded to a tapered steel core. Wing contours were generated by straight-line elements from the tip to the airfoil section at the root.

The control, triangular in shape and hinged about an axis canted forward at an angle of 45° with the root chord of the wing, had a constant-chord overhang balance of 71 percent of the maximum control chord measured rearward of and perpendicular to the hinge line. The overhang-balance area was 55 percent of the total control area. Two support hinges were used, one outboard on the wing and the other concealed in the housing of the bump. The overhang had an elliptical leading edge which was faired into the contour of the airfoil section rearward of the hinge line.

The model was mounted vertically on an electrical strain-gage balance enclosed within a chamber in the bump. The wing lift, drag, pitching moments, and rolling moments, and the flap hinge moments were measured with a calibrated electrical potentiometer. The balance chamber was sealed except for a small rectangular clearance hole through which an extension of the wing core passed. This hole was covered by the wing-root end plate, mounted approximately 0.05 inch above the surface of the bump.

TEST TECHNIQUE

The tests were made in the Langley high-speed 7- by 10-foot tunnel by means of an extension of the NACA wing-flow technique for attaining transonic speeds. The technique used involves testing the model in the local high-speed flow field induced over the curved surface of a bump mounted on the tunnel floor as described in reference 2.

Typical contours depicting local Mach number distribution over the test area of the bump with the model removed are shown in figure 2. The contours indicate a Mach number variation over the wing semispan of about 0.04 at low Mach numbers and from 0.05 to 0.06 in the higher ranges. The dashed lines at the root of the model in figure 2 indicate the estimated extent of the boundary layer with a local Mach number, at the dashed line, of approximately 95 percent of the maximum local

Mach number outside of the boundary layer. The effective test Mach number was obtained from contour charts similar to those presented in figure 2 by using the relationship

$$M = \frac{2}{S}\int_0^{b/2} cM_a \, dy$$

Force and moment data were obtained through a Mach number range of 0.60 to 1.18 and an angle-of-attack range of -2° to 6° with a few tests extended to 8°. Control deflections investigated were from -10° to 10°. The variation of mean Reynolds number with Mach number is presented in figure 3 and varied from 1,100,000 to 1,500,000. The boundaries of the figure are indications of the possible range in Reynolds number caused by variations in test conditions.

CORRECTIONS

The lift, drag, and pitching moments represent data for the complete wing with controls mounted on both semispans.

Rolling moment of the semispan wing is presented as gross rolling-moment coefficient. No reflection-plane corrections were applied to the rolling-moment data because of the unconventional arrangement of the control surface, balance, and skewed hinge axis and because no corrections are available that apply in the transonic and supersonic speed ranges. It is of interest to note, however, that the corrections applicable to conventional wing-aileron configurations at the lower speeds of around $M = 0.3$ reduce the incremental rolling-moment coefficients due to control deflections approximately 40 percent.

The peculiarity of the design of the wing necessitated the use of a relatively long and thin control spar extension at the inboard hinge which permitted measurable deflection in torsion when loads were applied. Static loading tests indicated this deflection to be a direct function of the hinge moment applied, and corrections were made accordingly. The wing proper, when statically loaded to anticipated air-load limits, was found to have negligible deflection in torsion and bending; therefore no corrections were applied.

RESULTS AND DISCUSSION

The variation of lift, drag, pitching-moment, hinge-moment, and rolling-moment coefficients with control deflection for each Mach number

investigated is presented in figures 4 to 11. Although the model employed a symmetrical airfoil section, asymmetry of data for the positive and negative ranges of control deflection is apparent in figures 4 to 11. This asymmetry can be attributed to small inaccuracies of construction and to slight errors in setting angle of attack and control deflection during the test.

Examination of figures 4 to 11 indicates that the flap was effective in producing changes in lift and pitching moment throughout the range of Mach numbers investigated. The variation of lift and pitching moment with control deflection was nonlinear and increased in the higher ranges of deflection.

The values of drag coefficient and gross rolling-moment coefficient produced at a specific control deflection generally increased with increase in Mach number up to $M = 1.0$ and decreased slightly from $M = 1.0$ to $M = 1.18$.

The control was overbalanced at small deflections at all Mach numbers (figs. 4 to 11). Increase in Mach number increased the degree of overbalance and extended it over a slightly wider range of deflections.

The variation of hinge-moment coefficient with angle of attack at a control deflection of 0° for all Mach numbers investigated is presented in figure 12. The control was overbalanced in the low ranges of angle of attack at all Mach numbers investigated. At Mach numbers above $M = 1.0$, the region of overbalance extended over the complete range of angle of attack.

It is appropriate at this point to note that the overbalance of the control can probably be attributed to the fact that the spanwise loading of a triangular wing, rather than being fully elliptical as predicted in reference 1, falls off appreciably at the tips. This loss of tip loading, unpredicted in the theory, could account for the overbalance at low angles of attack. As the angle of attack of a triangular wing is further increased, the centers of pressure at chordwise sections near the tip move progressively rearward, as shown in reference 3, with the consequent reduction in overbalance of the control under discussion.

The model used in this investigation was somewhat similar to a model used in the investigation reported in reference 4, as can be noted on the comparative sketches of the two models in figure 13. The controls used on the two models are considered representative of a general type, one aerodynamically balanced and the other unbalanced, in that the surfaces rearward of the skewed hinge axes are generally similar.

[redacted]

A comparison of the incremental lift coefficient at various control deflections at zero angle of attack for several Mach numbers is presented against hinge-moment coefficient in figure 14 for the balanced control and for the plain triangular control of reference 4. The balanced control was tested at Reynolds numbers from 1,100,000 to 1,500,000 while the plain, unbalanced control of reference 4 was tested at a constant Reynolds number of 3,200,000. For this comparison, control deflections of the wing of reference 4 were considered to be measured in a plane perpendicular to the control hinge axis.

An examination of figure 14 shows that the balanced triangular control was more effective in producing lift for a given value of hinge-moment coefficient than was the plain control. This, however, may be partly attributable to the nonlinearity of the hinge-moment characteristics of the former. This trend of increased effectiveness for the balanced control became more pronounced with increase in Mach number.

The control effectiveness parameters presented against Mach number in figure 15 were obtained from figures 4 to 11. The linear variations of aerodynamic characteristics were generally contained within a control deflection range of $\pm 2^\circ$, and the slopes presented were obtained within this range. It should be noted that this linear range of deflection was within the region of control overbalance. Presented as comparisons with the control parameters of the balanced triangular control are similar control parameters of the plain control of reference 4.

Lift effectiveness C_{L_δ} and pitching-moment effectiveness C_{m_δ} of the balanced control increased up to high subsonic speeds, above which the effectiveness decreased rapidly with further increase in Mach number. The values of C_{L_δ} and C_{m_δ} of the plain control exhibited a lesser increase with Mach number and generally were approximately 25 percent of the corresponding values for the balanced control.

The values of C_{h_δ} and C_{h_α} for the balanced control became more positive with increase in Mach number up to $M = 0.95$ and $M = 1.0$, respectively, and then rapidly decreased until M equaled 1.18; whereas C_{h_δ} and C_{h_α} for the plain control increased negatively with increase in Mach number.

Rolling-moment effectiveness C_{l_δ} increased except for a sharp reversal in trend in the transonic speed range.

[redacted]

CONCLUDING REMARKS

The results of the investigation on the balanced control indicate the plausibility of incorporating an aerodynamic balance on a triangular control of a delta wing that will increase lift effectiveness of the control while maintaining hinge moments within practical limits.

The balanced control for all aerodynamic characteristics studied was more affected by compressibility than was a plain control of generally similar plan form.

Langley Aeronautical Laboratory
National Advisory Committee for Aeronautics
Langley Field, Va.

REFERENCES

1. Jones, Robert T.: Properties of Low-Aspect-Ratio Pointed Wings at Speeds below and above the Speed of Sound. NACA Rep. 835, 1946.

2. Schneiter, Leslie E., and Ziff, Howard L.: Preliminary Investigation of Spoiler Lateral Control on a 42° Sweptback Wing at Transonic Speeds. NACA RM L7F19, 1947.

3. Anderson, Adrien E.: Chordwise and Spanwise Loadings Measured at Low Speed on Large Triangular Wings. NACA RM A9B17, 1949.

4. Kolbe, Carl D., and Tinling, Bruce E.: Tests of a Triangular Wing of Aspect Ratio 2 in the Ames 12-Foot Pressure Wind Tunnel. III - The Effectiveness and Hinge Moments of a Skewed Wing-Tip Flap. NACA RM A8E21, 1948.

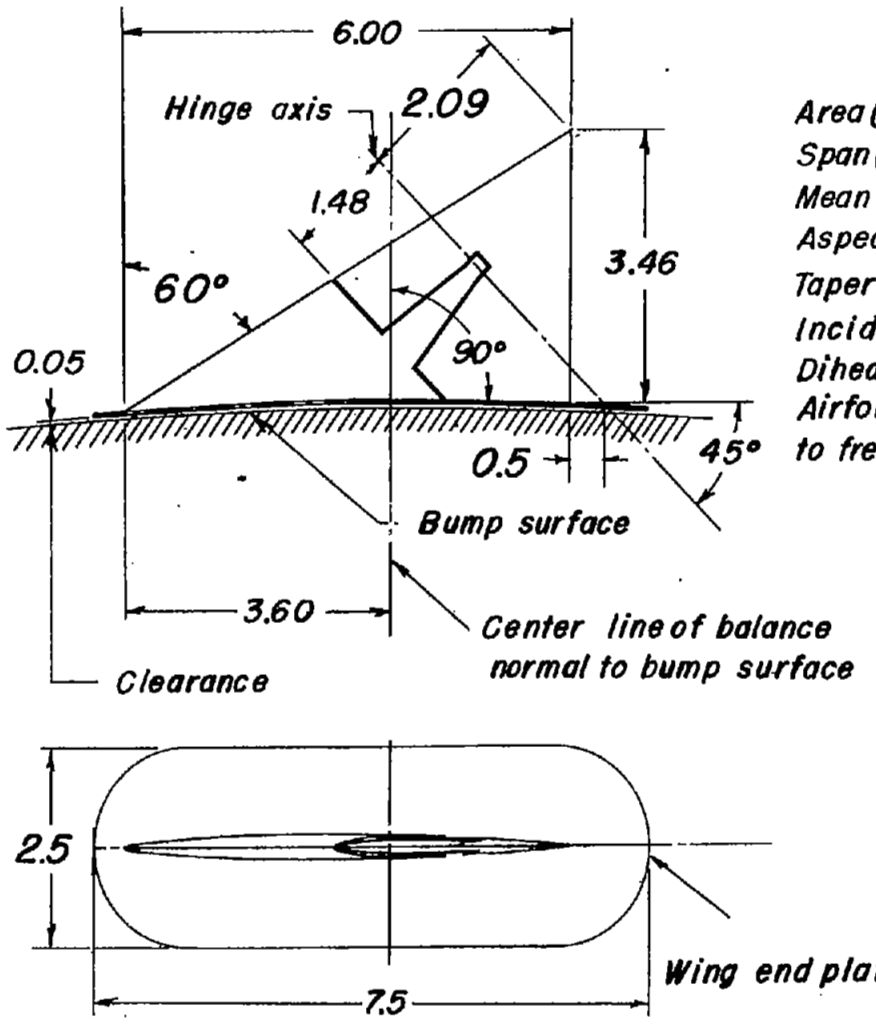

TABULATED WING DATA

Area (twice semispan)	0.144 sq ft
Span (twice semispan)	0.578 ft
Mean aerodynamic chord	0.333 ft
Aspect ratio	2.31
Taper ratio	0
Incidence	0°
Dihedral	0°
Airfoil section parallel to free air stream	NACA 65 -006

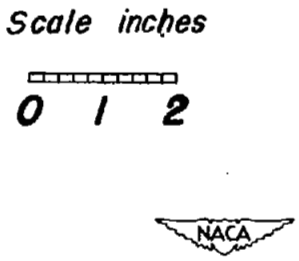

Figure 1.—General arrangement of model of 60° delta wing with triangular flap and large overhang balance. (All dimensions in inches.)

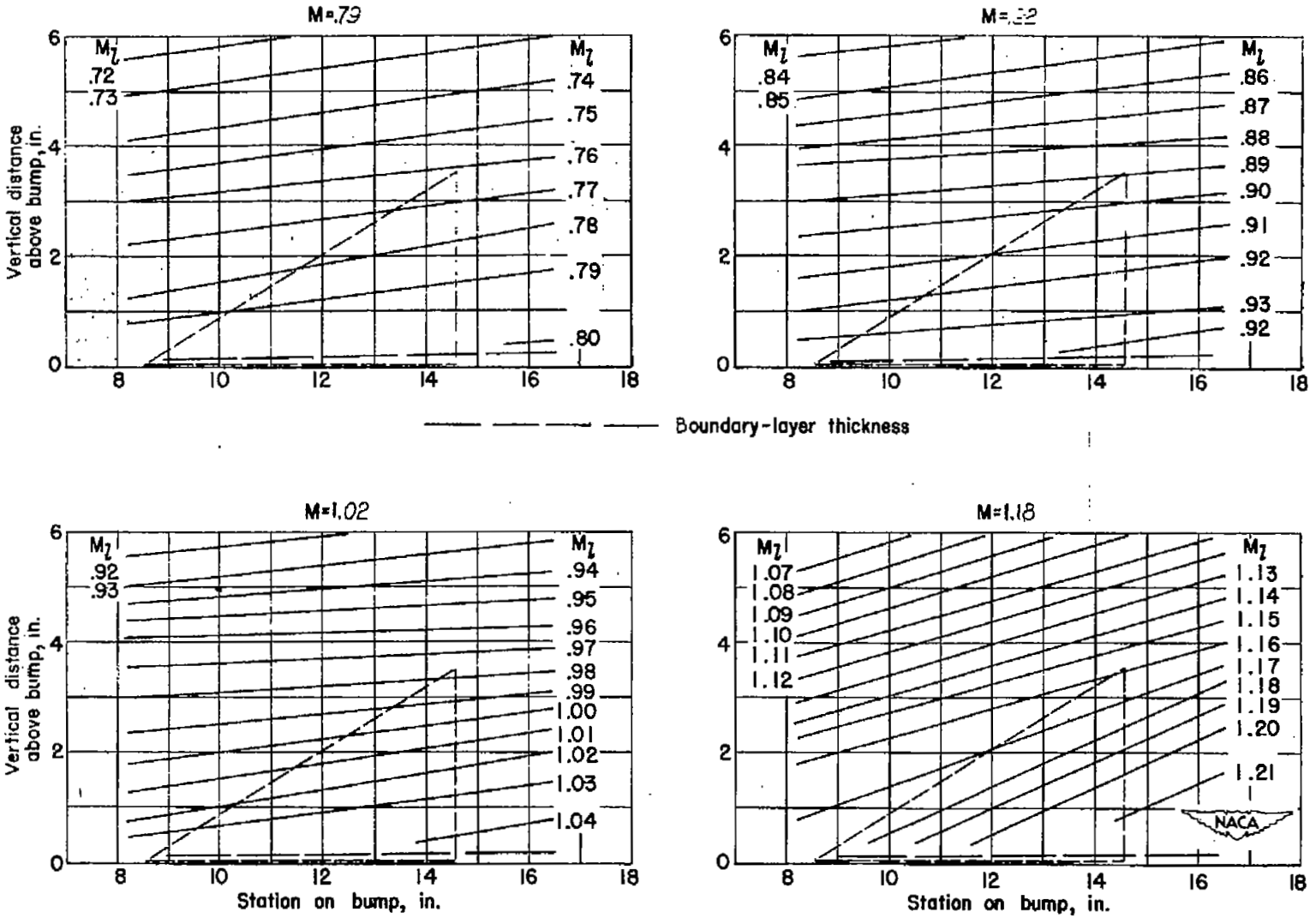

Figure 2 .- Typical Mach number contours over transonic bump in region of model location.

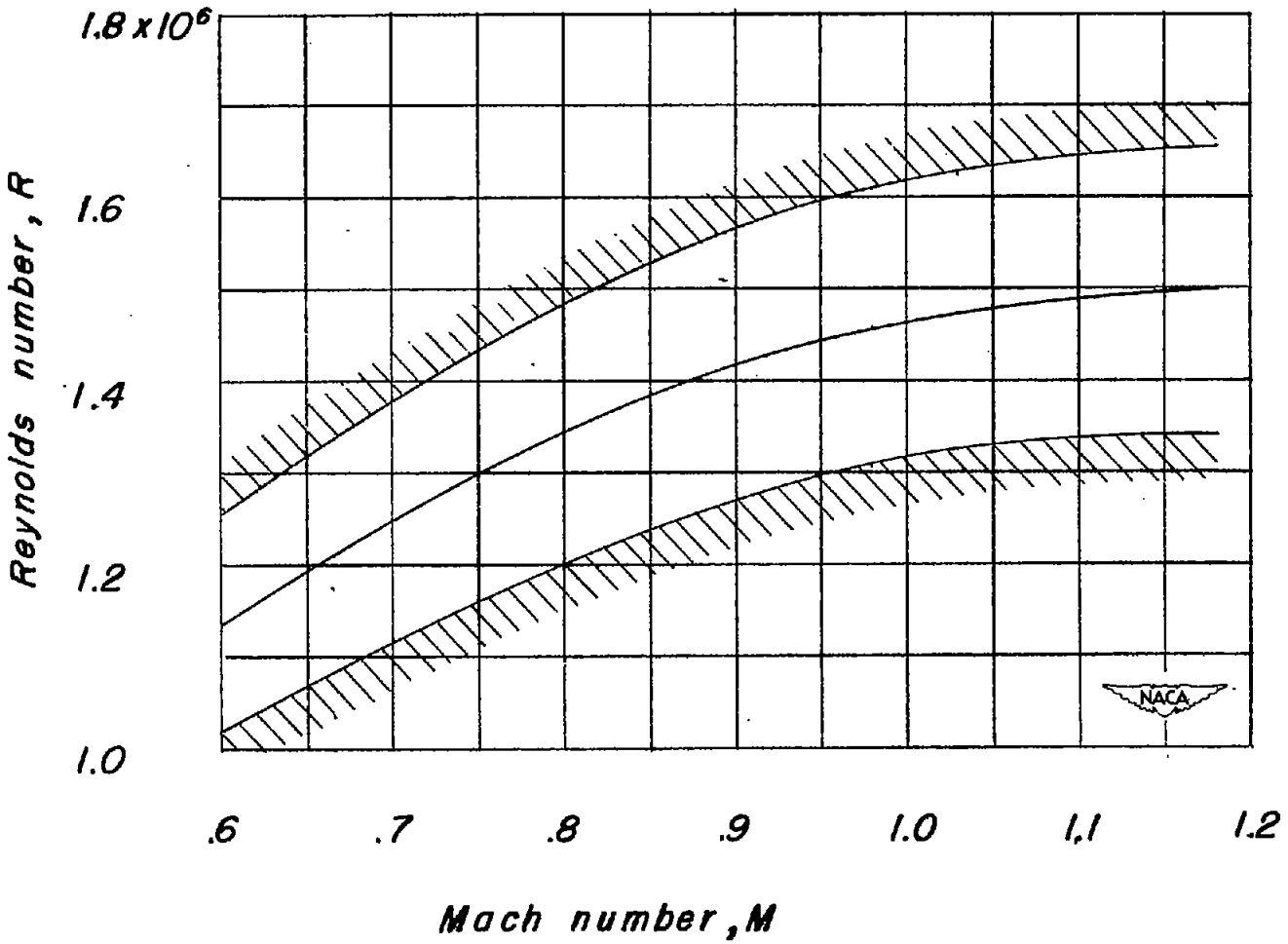

Figure 3.—Variation of test Reynolds number with Mach number for model of a 60° delta wing with triangular flap and overhang balance, aspect ratio 2.31, taper ratio 0, and NACA 65-006 airfoil.

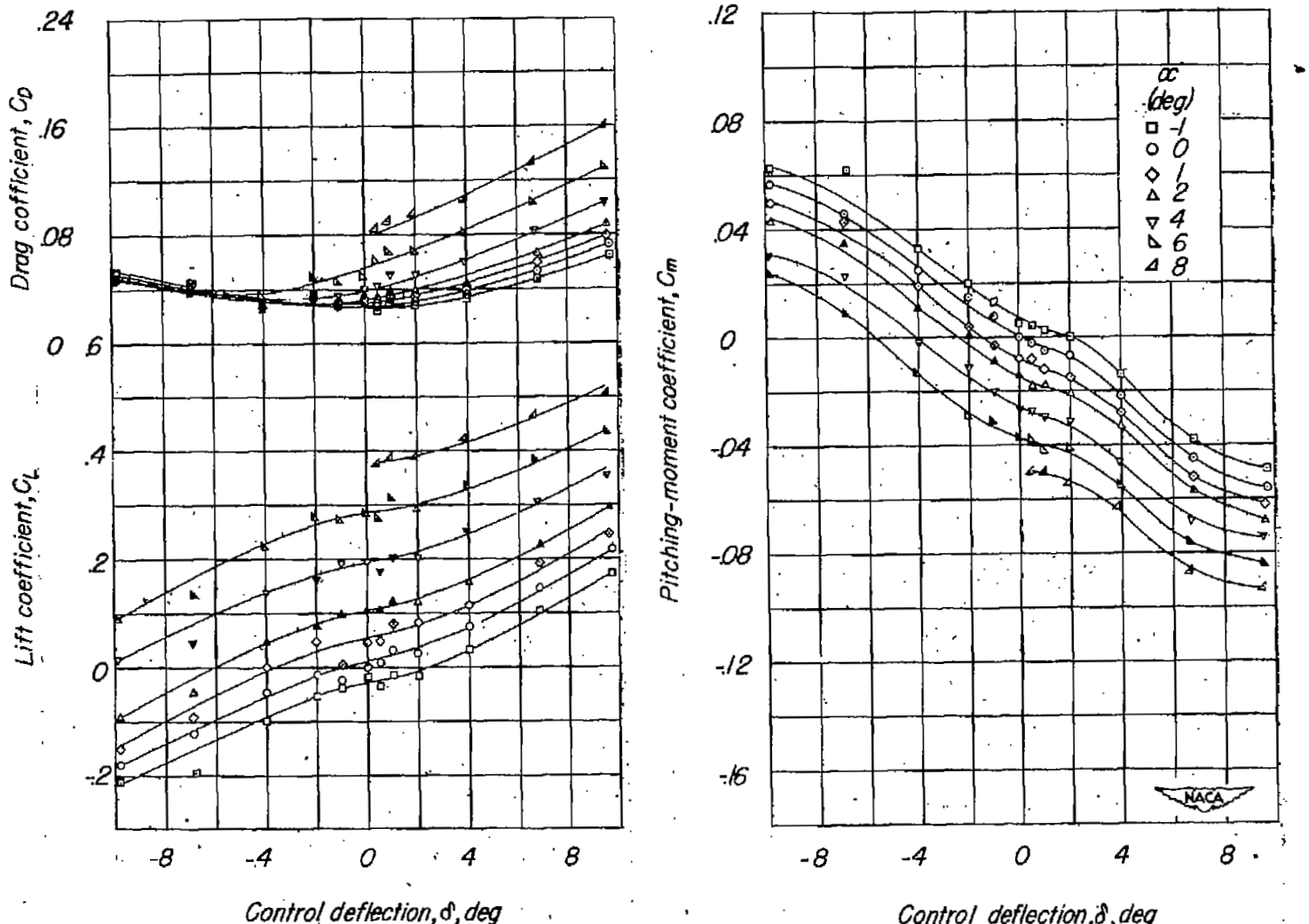

Figure 4.—Aerodynamic characteristics of model of 60° delta wing with triangular flap and overhang balance, aspect ratio 2.31, taper ratio 0, and NACA 65 -006 airfoil. M=0.6.

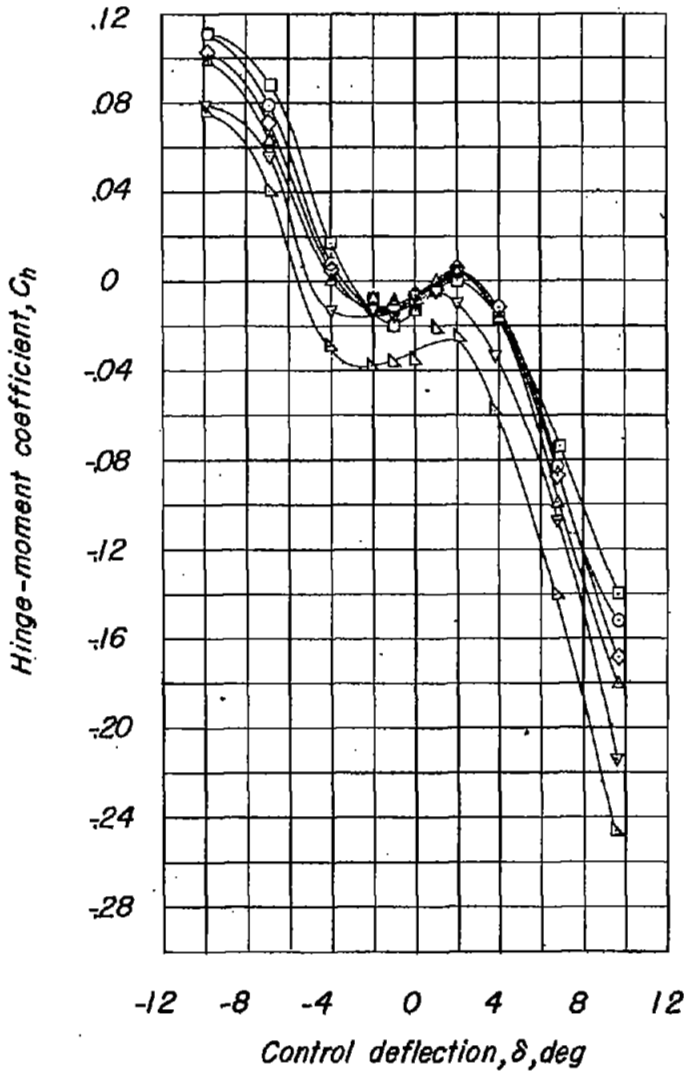

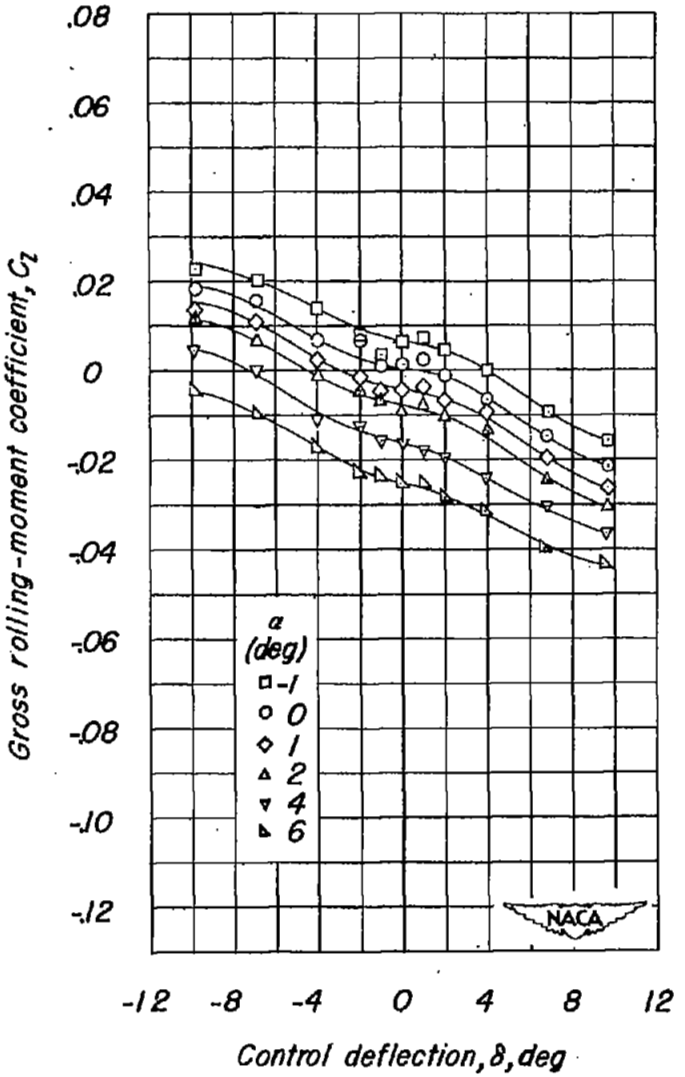

Figure 4.—Concluded.

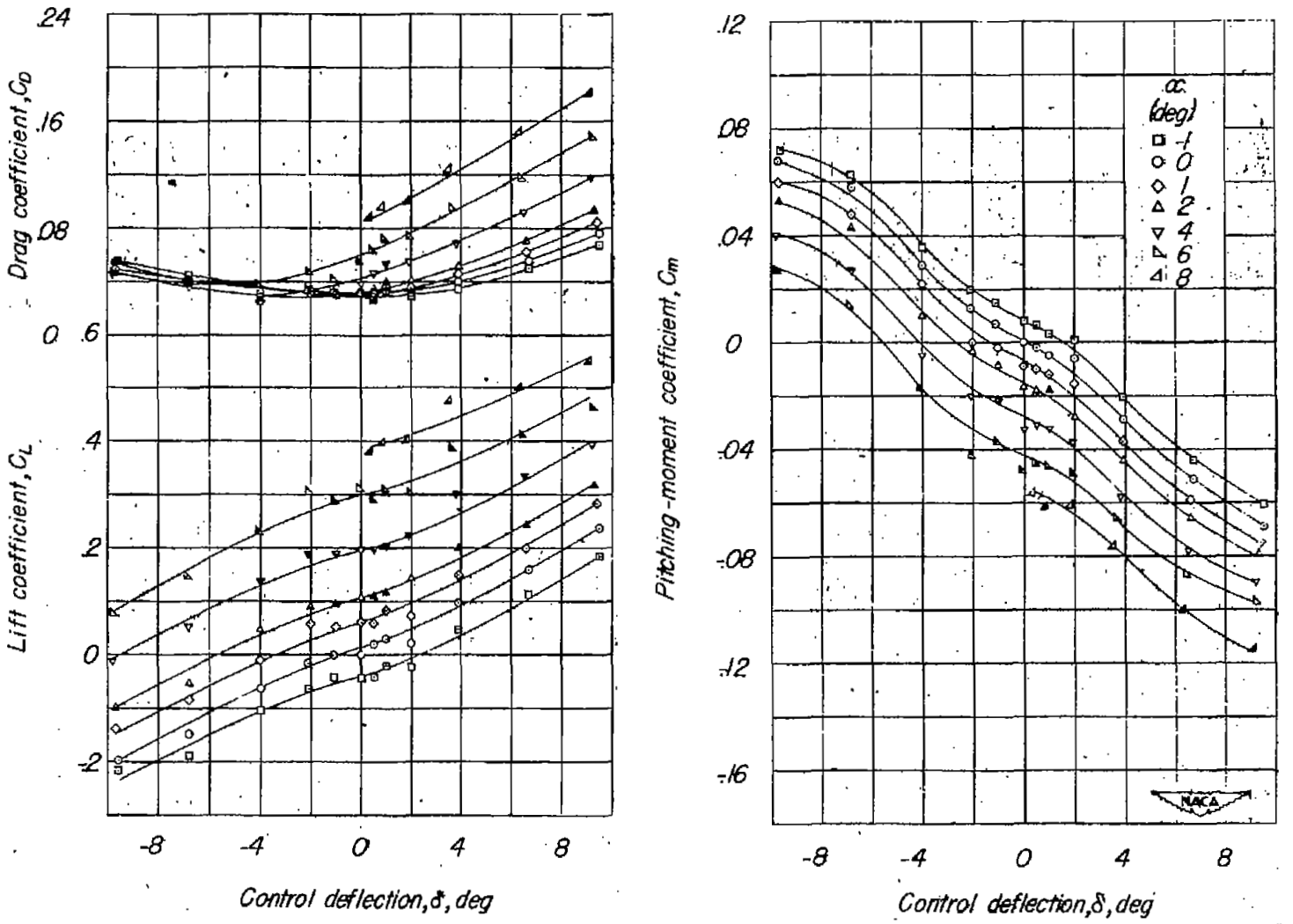

Figure 5.—Aerodynamic characteristics of model of 60° delta wing with triangular flap and overhang balance, aspect ratio 2.31, taper ratio 0, and NACA 65 -006 airfoil. M = 0.8.

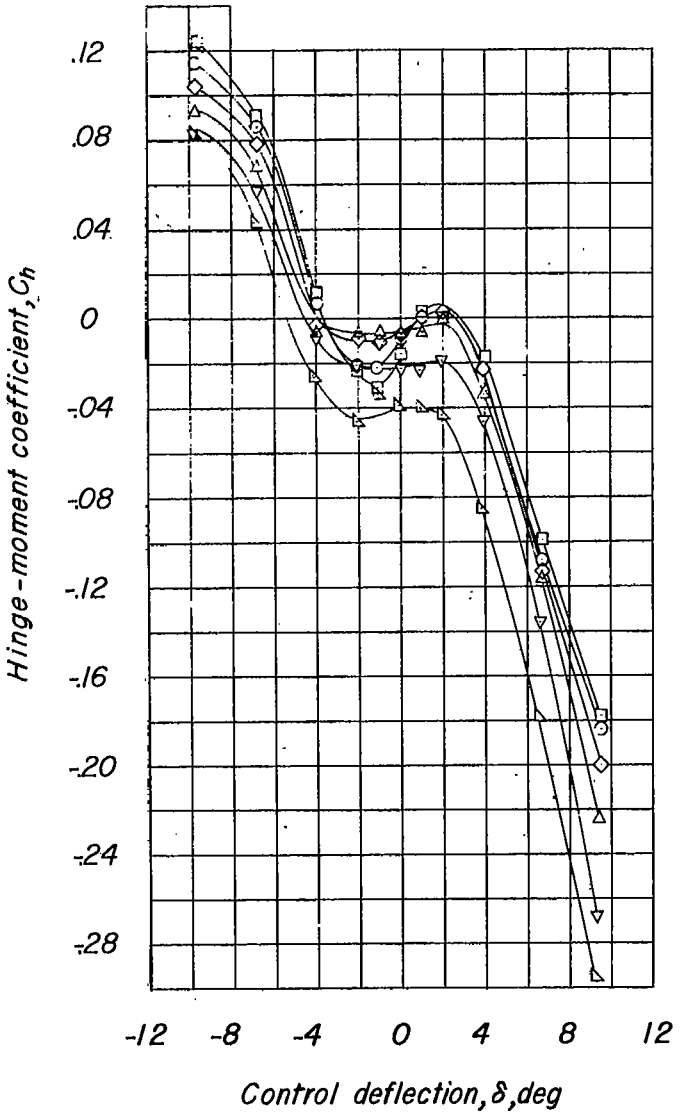

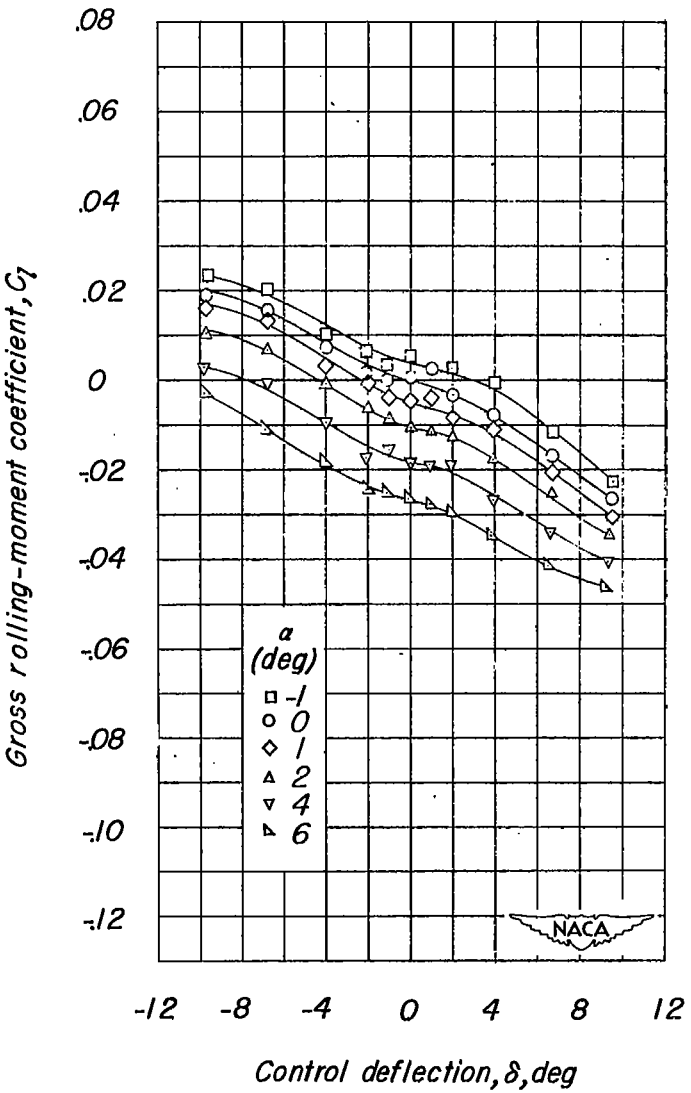

Figure 5.—Concluded

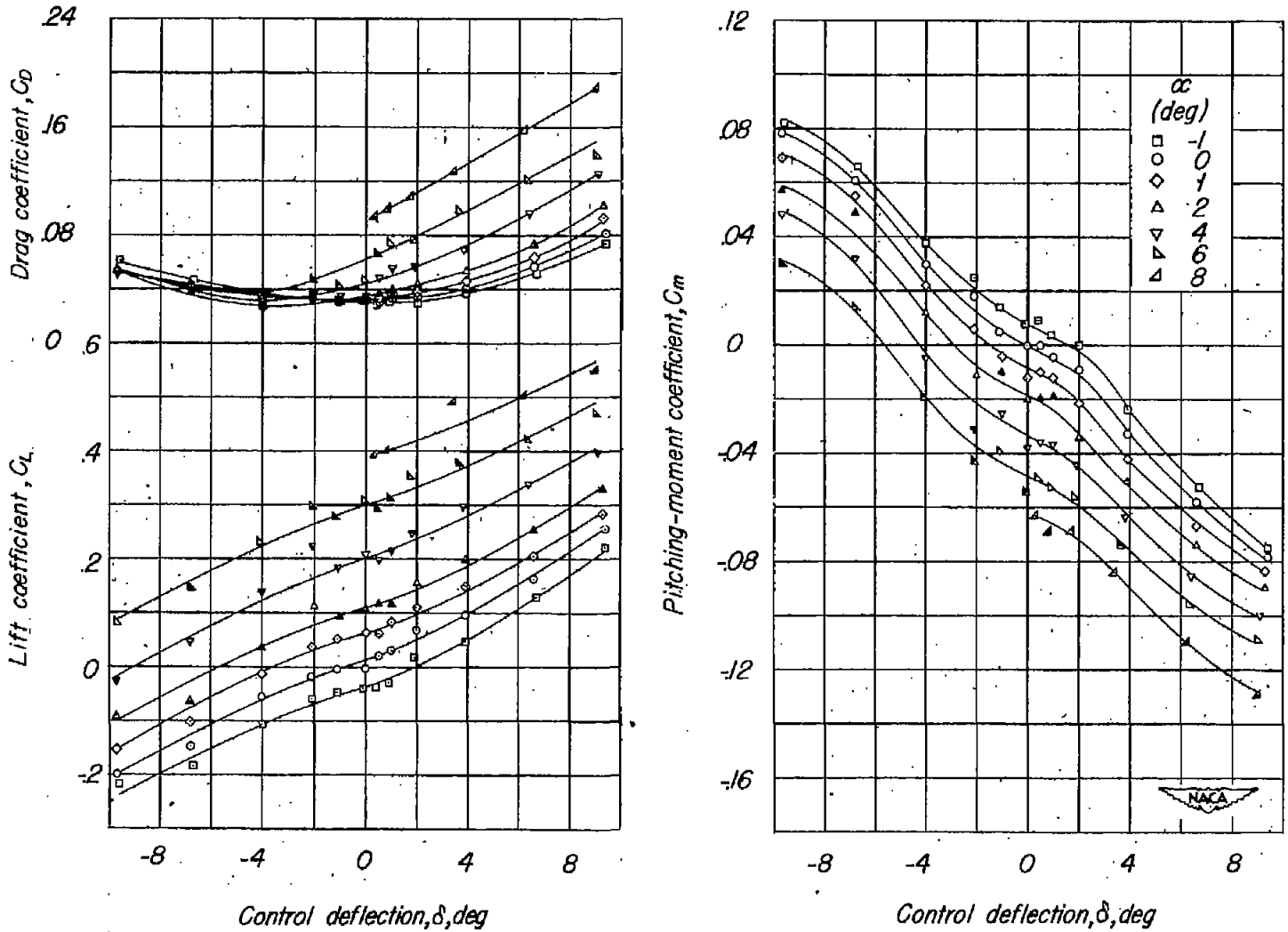

Figure 6.—Aerodynamic characteristics of model of 60° delta wing with triangular flap and overhang balance, aspect ratio 2.31, taper ratio 0, and NACA 65 -006 airfoil. M = 0.9.

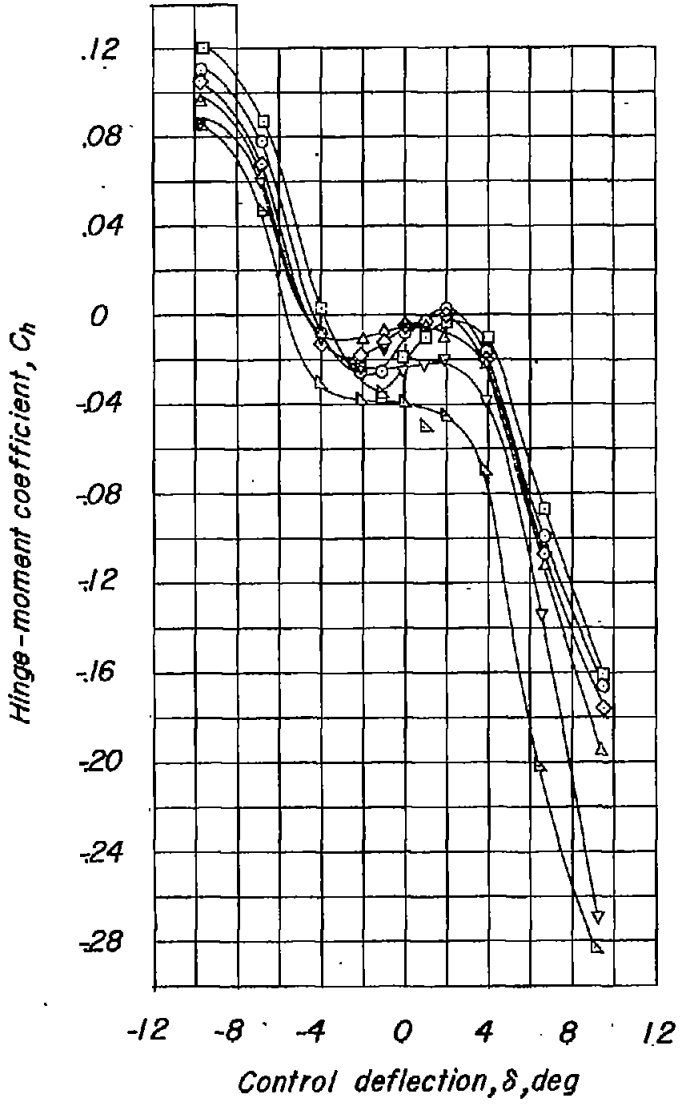

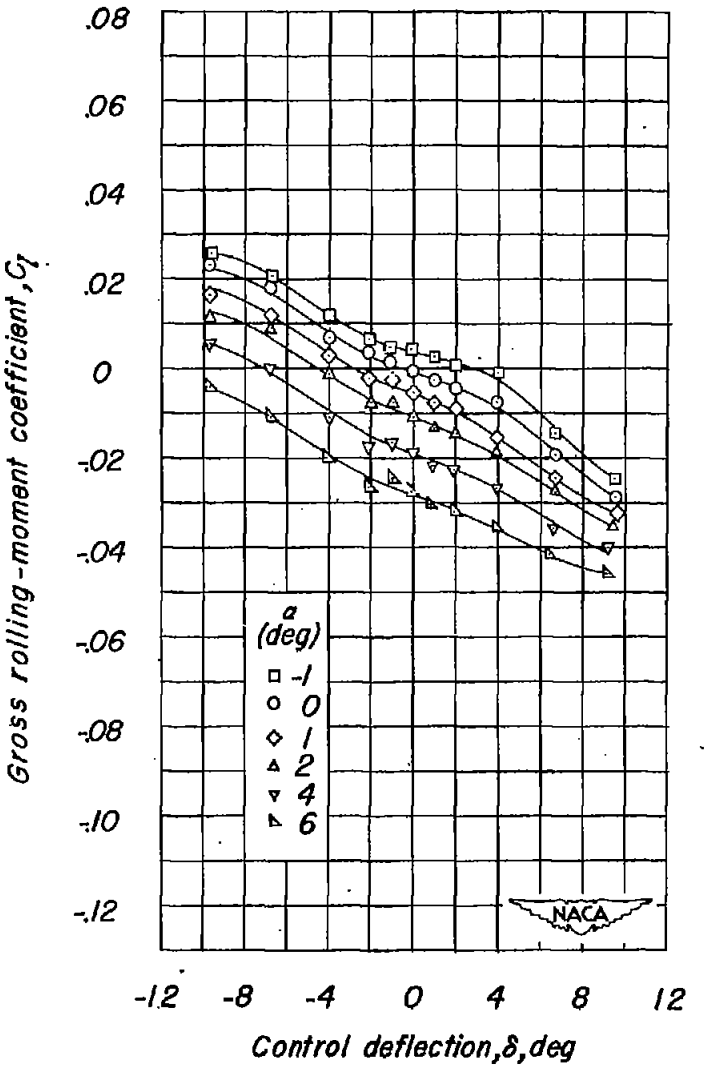

Figure 6.— Concluded.

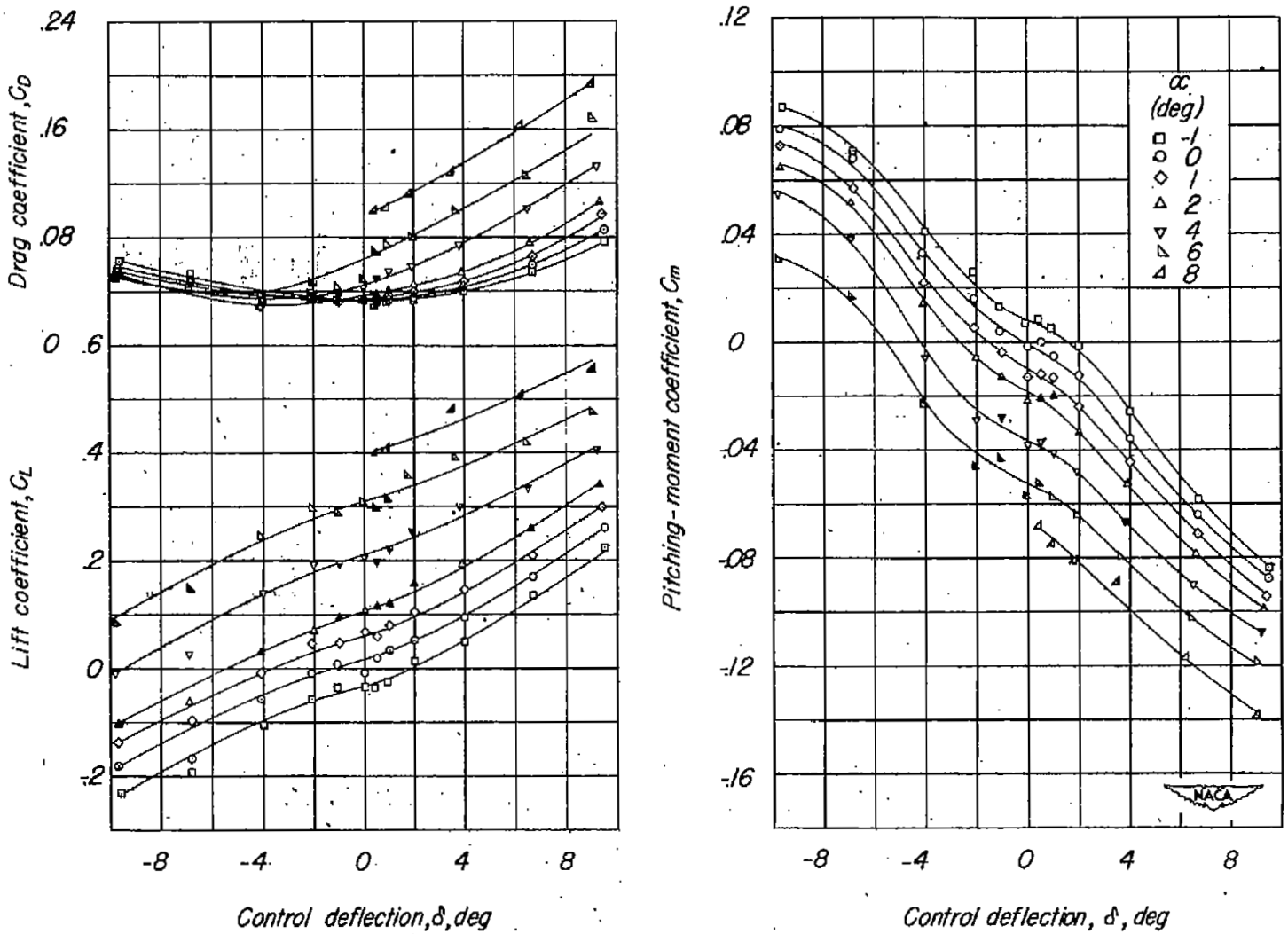

Figure 7.—Aerodynamic characteristics of model of 60° delta wing with triangular flap and overhang balance, aspect ratio 2.31, taper ratio 0, and NACA 65 -006 airfoil. M = 095.

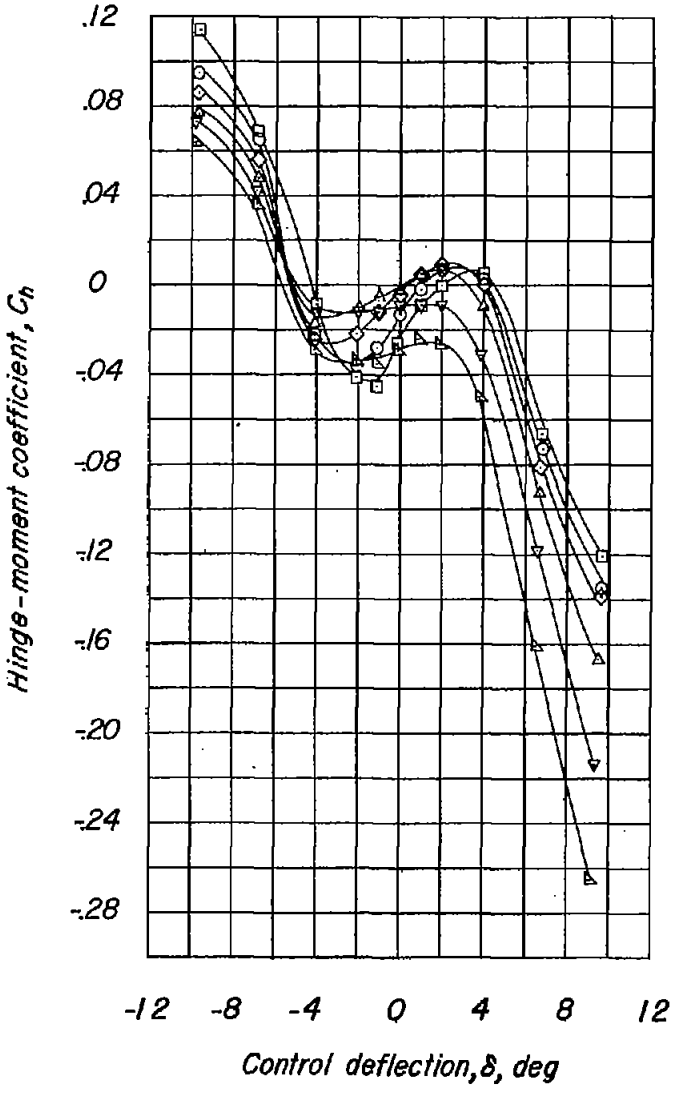

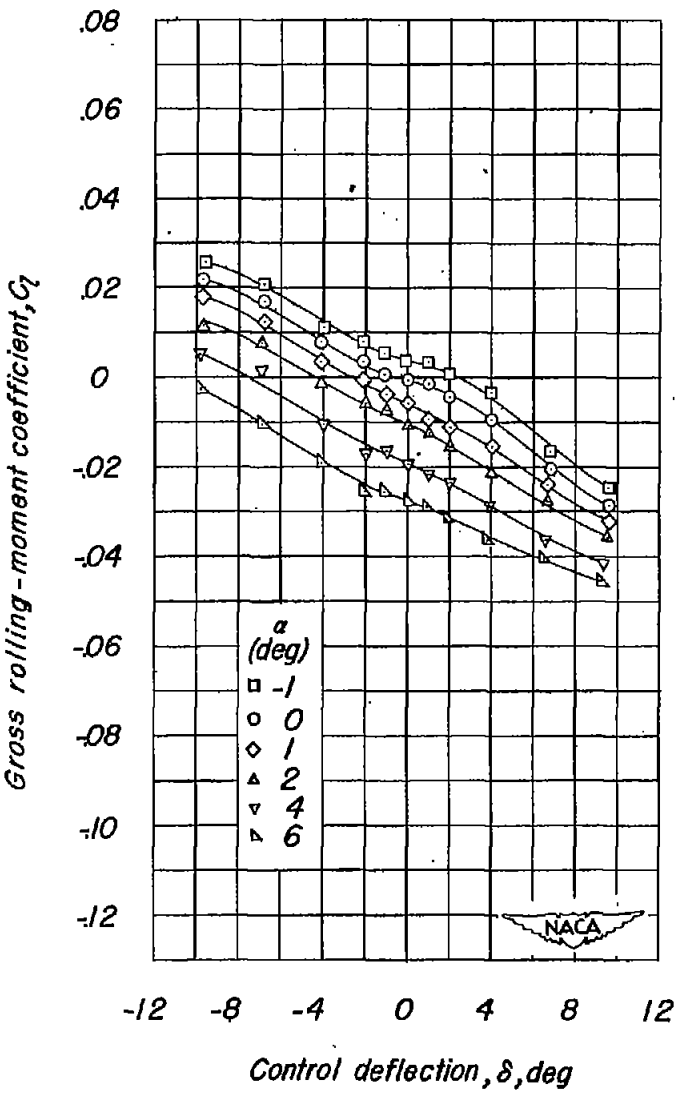

Figure 7.— Concluded.

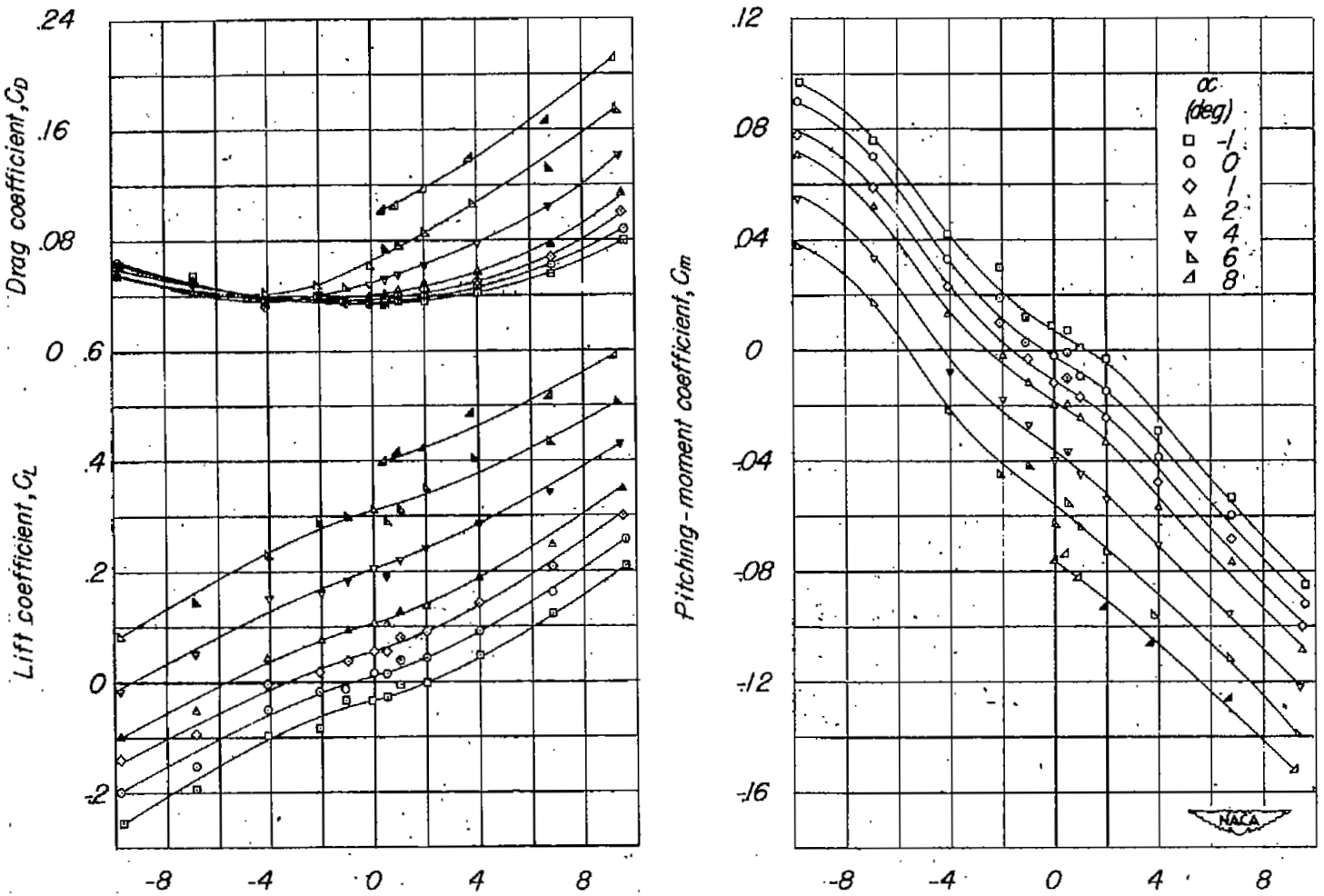

Figure 8.—Aerodynamic characteristics of model of 60° delta wing with triangular flap and overhang balance, aspect ratio 2.31, taper ratio 0, and NACA 65-006 airfoil. M=1.00.

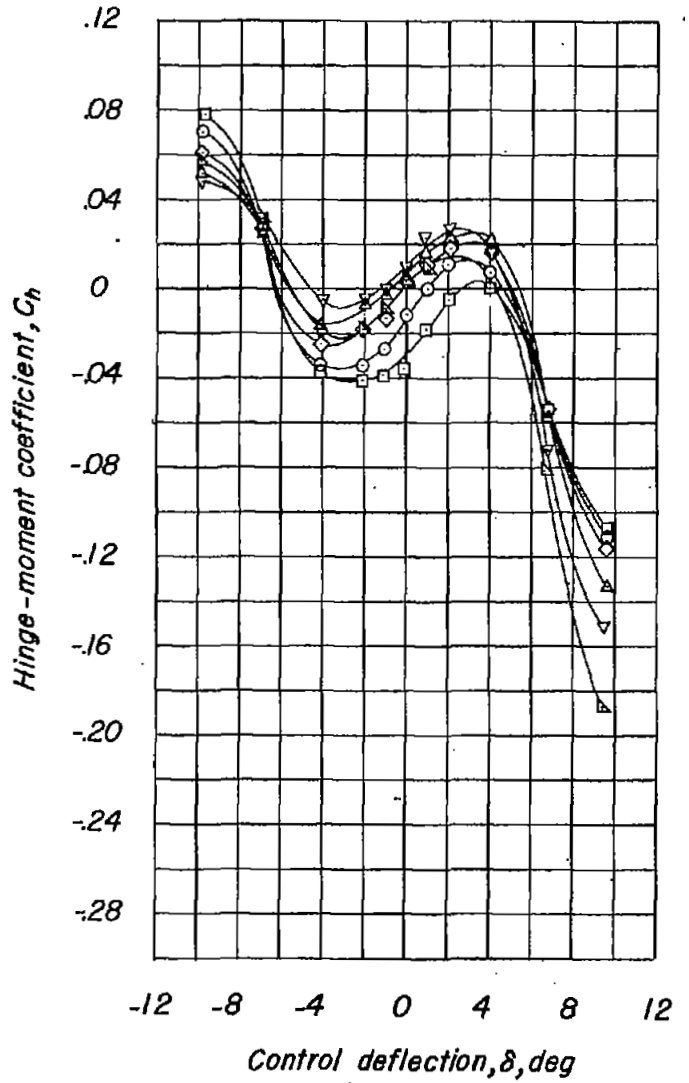

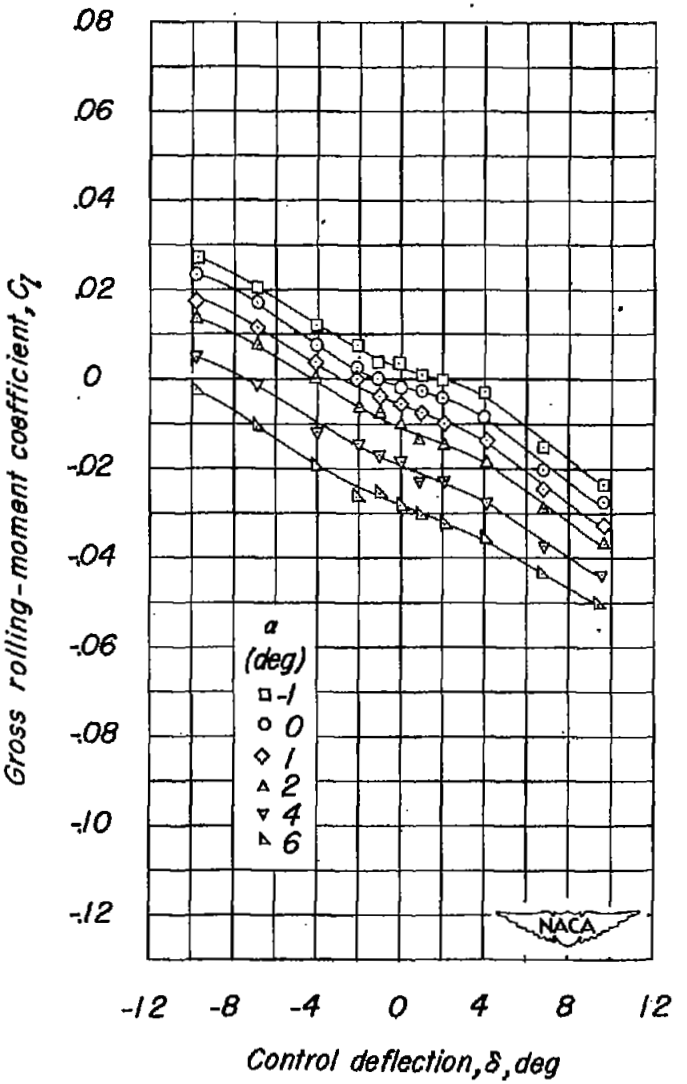

Figure 8.— Concluded.

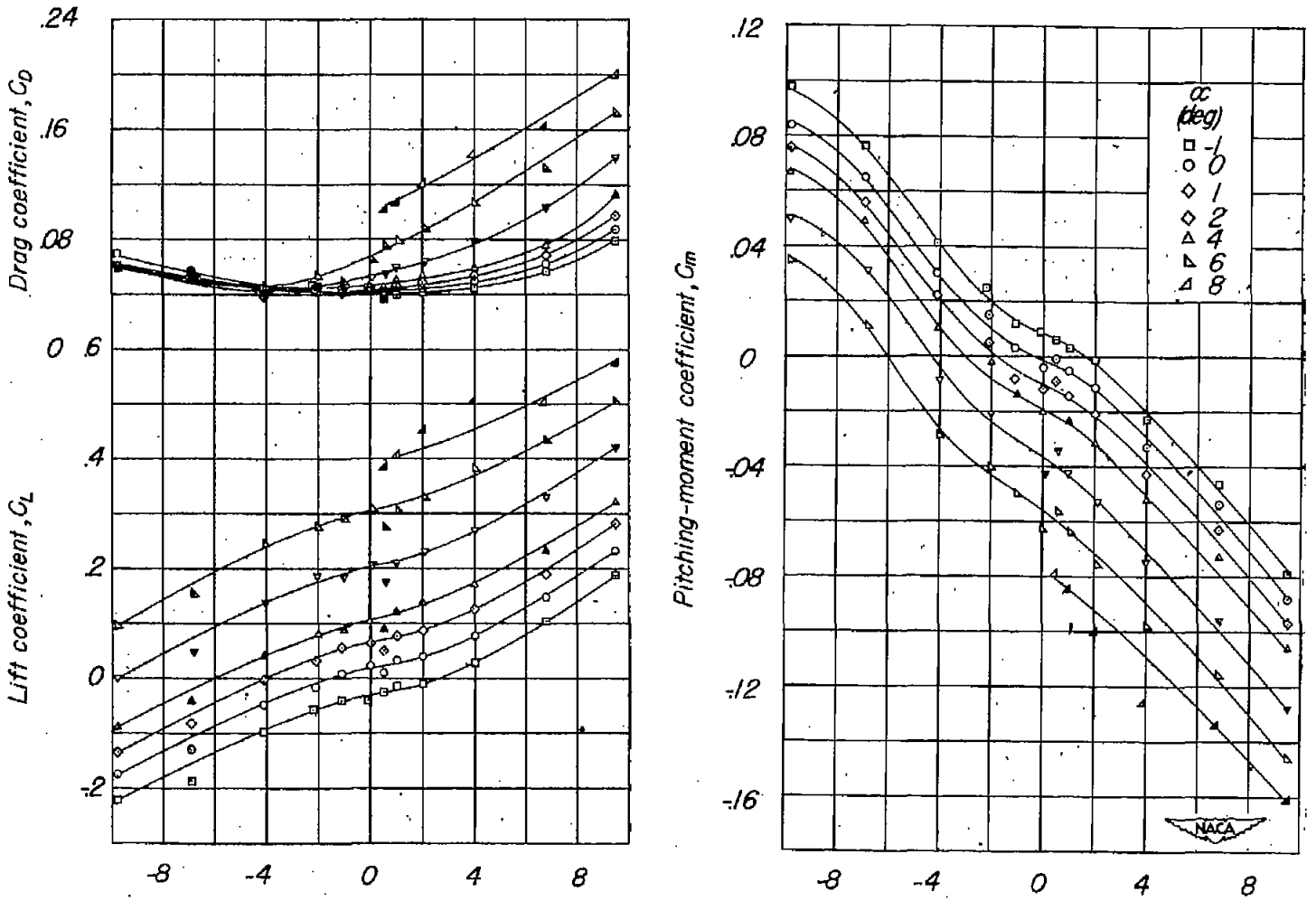

Figure 9.—Aerodynamic characteristics of model of 60° delta wing with triangular flap and overhang balance, aspect ratio 2.31, taper ratio 0, and NACA 65-006 airfoil. M=1.05.

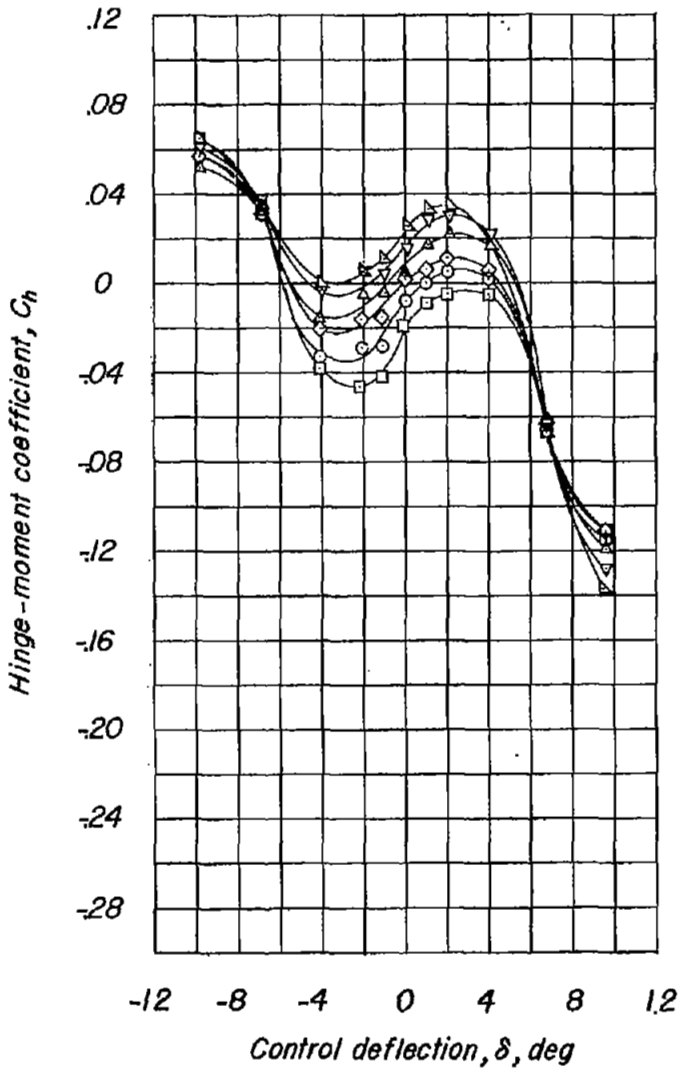

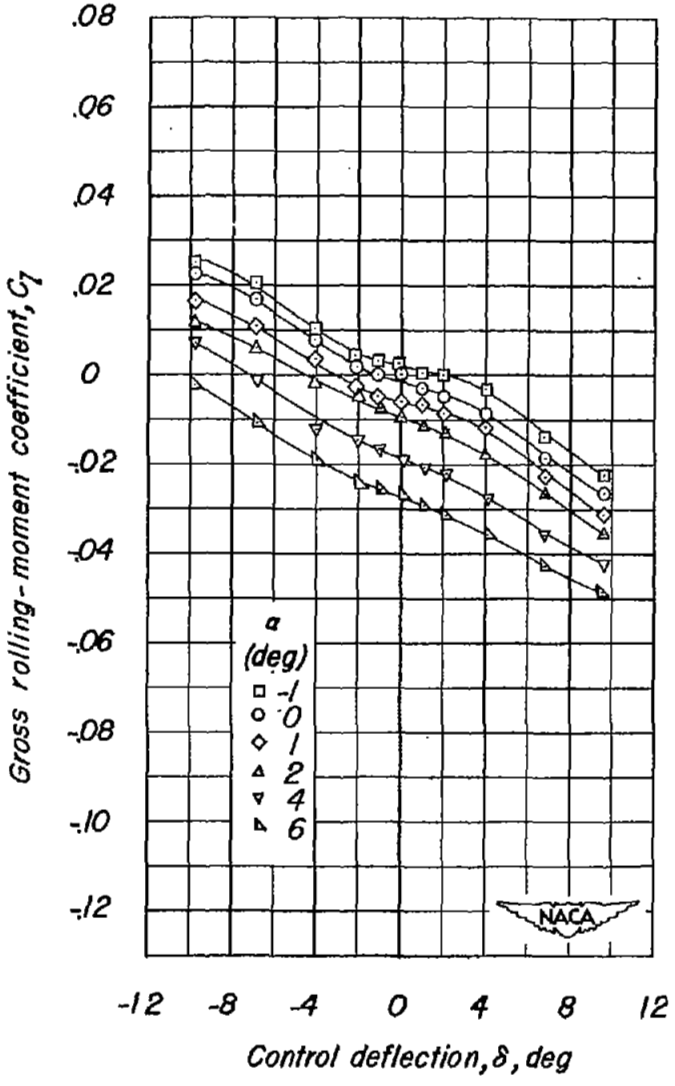

Figure 9.— Concluded.

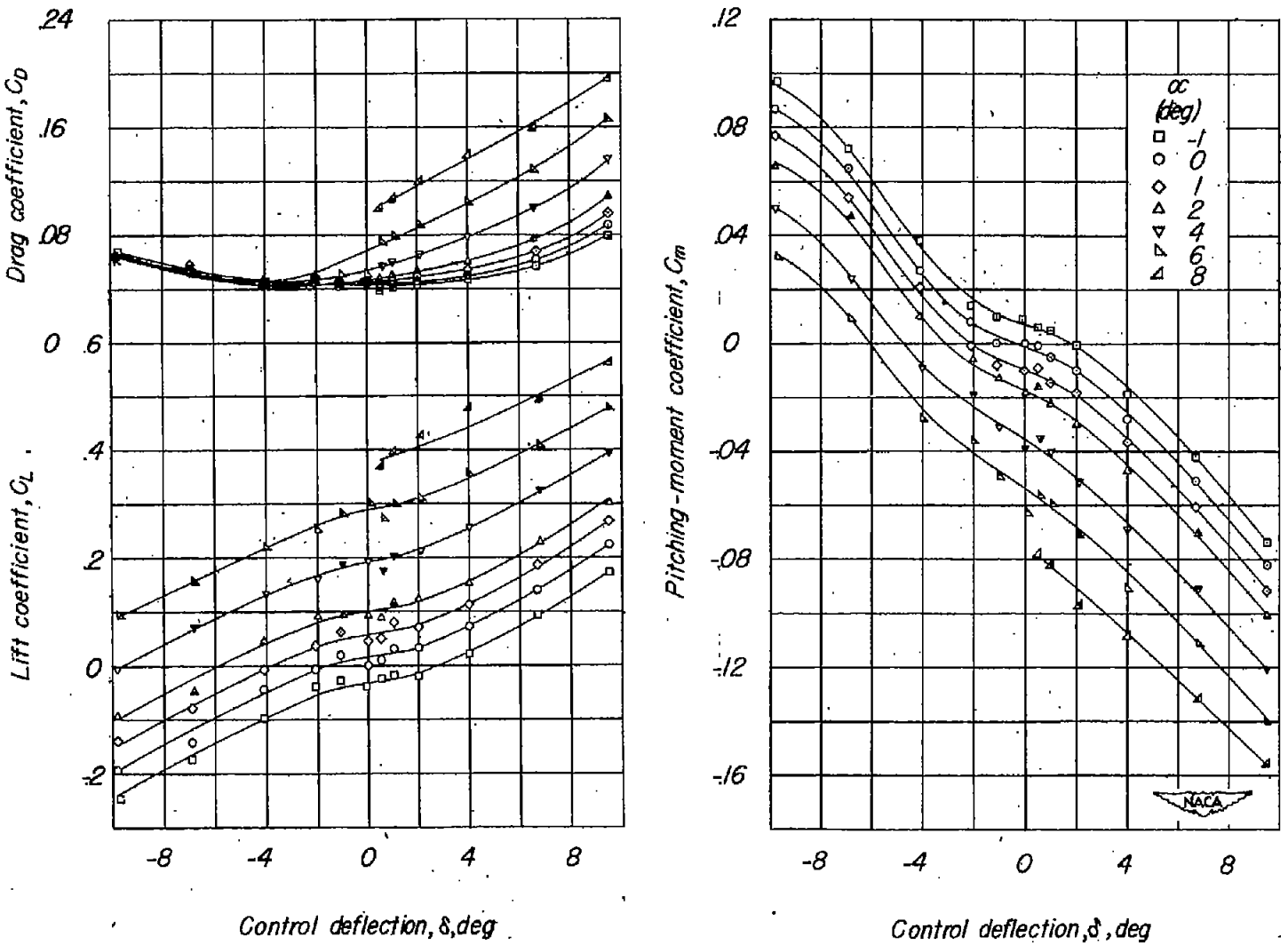

Figure 10.—Aerodynamic characteristics of model of 60° deltawing with triangular flap and overhang balance, aspect ratio 2.31, taper ratio 0, and NACA 65-006 airfoil. M=1.10.

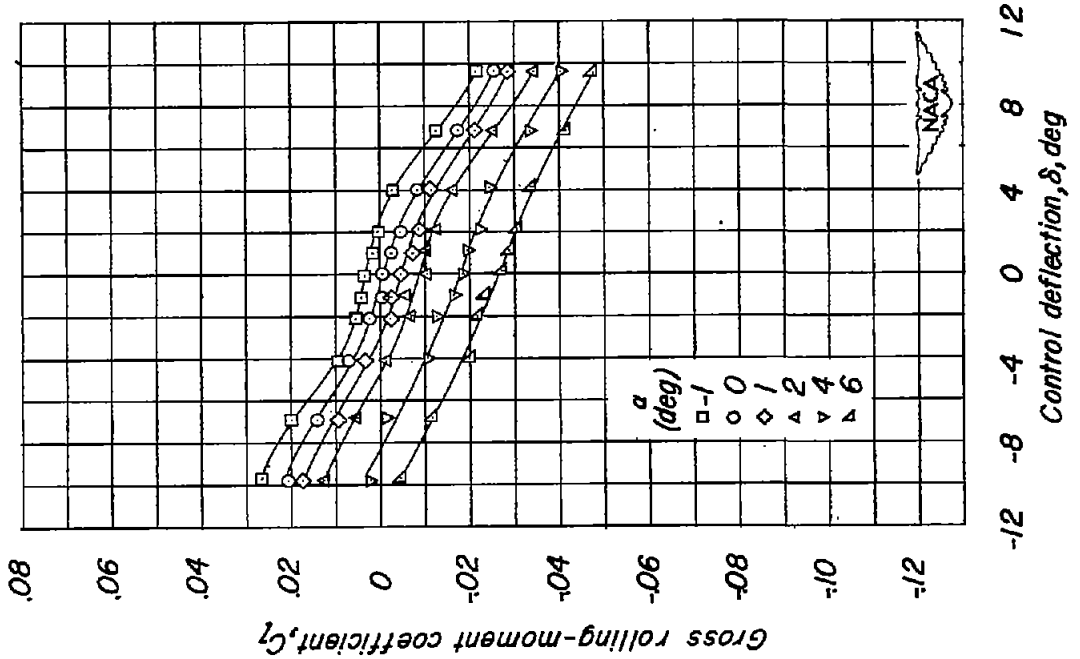

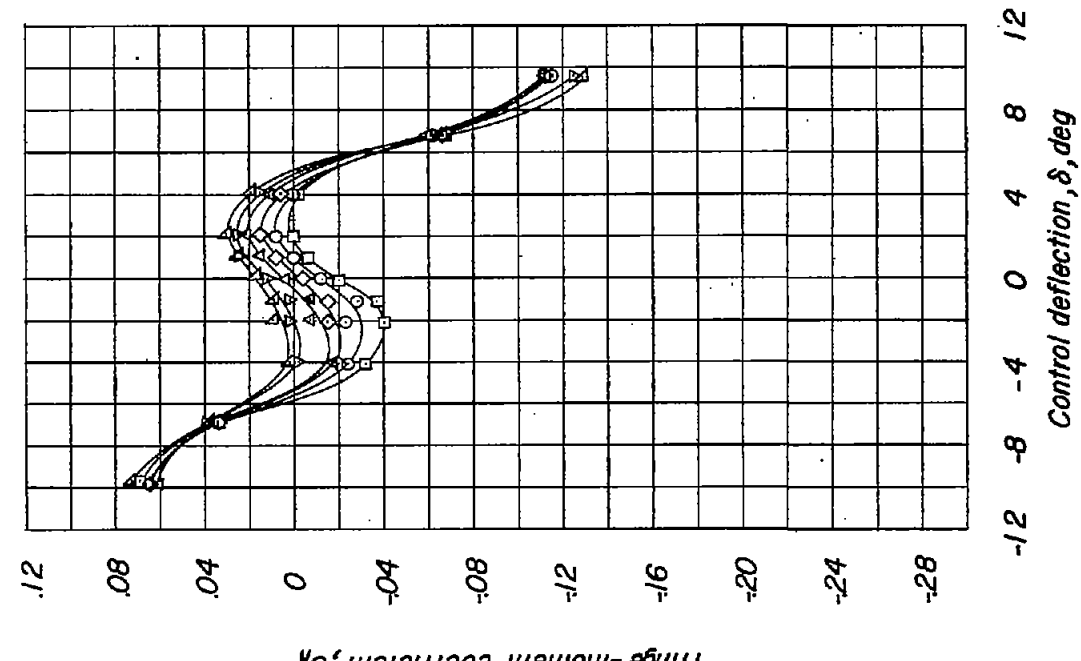

Figure 10.—Concluded.

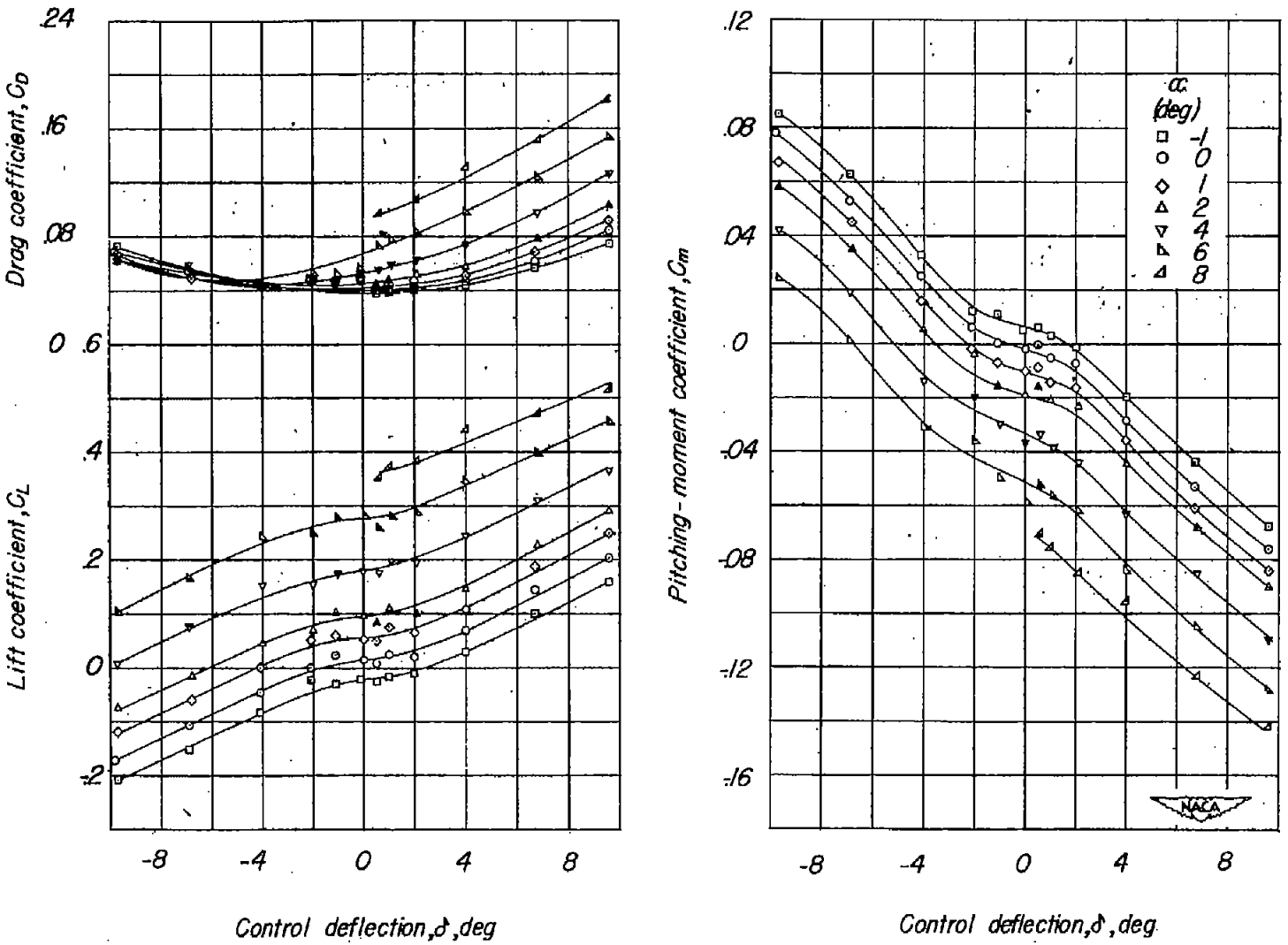

Figure 11.— Aerodynamic characteristics of model of 60° delta wing with triangular flap and overhang balance, aspect ratio 2.31, taper ratio 0, and 65 - 006 airfoil M = 1.18.

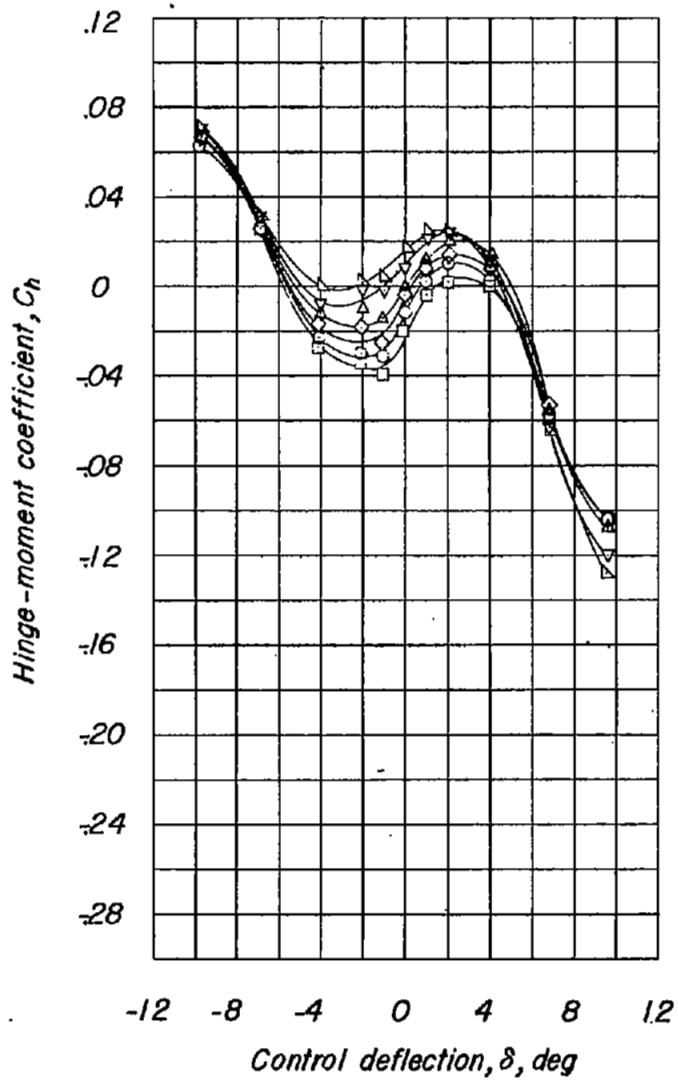

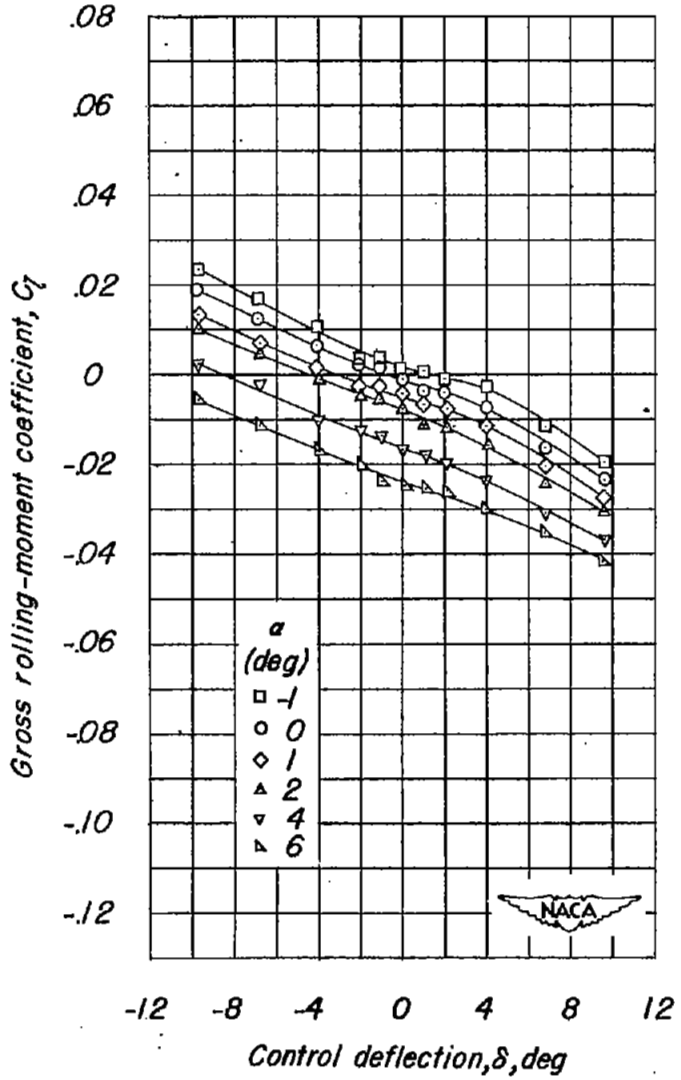

Figure 11.—Concluded.

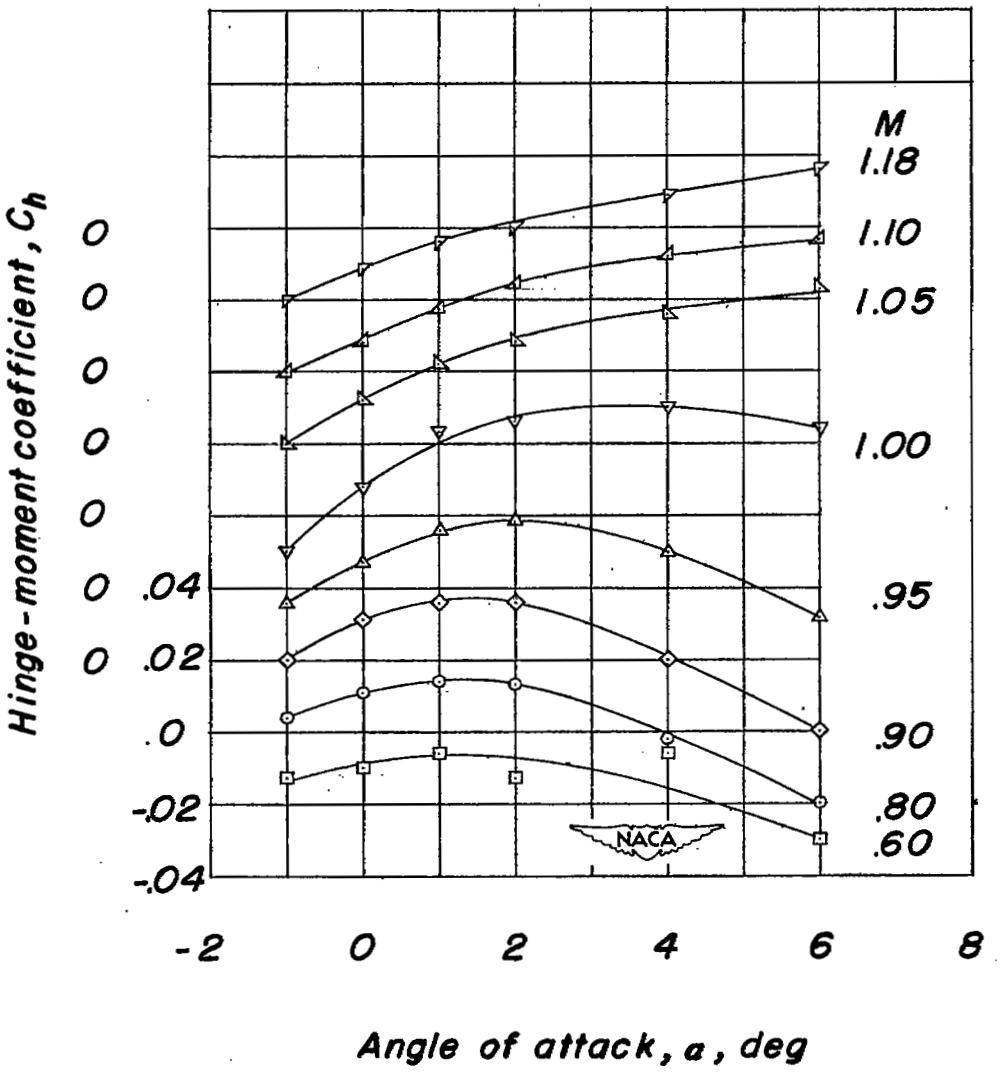

Figure 12.-- The variation of hinge-moment coefficient with angle of attack for various Mach numbers. $\delta = 0°$.

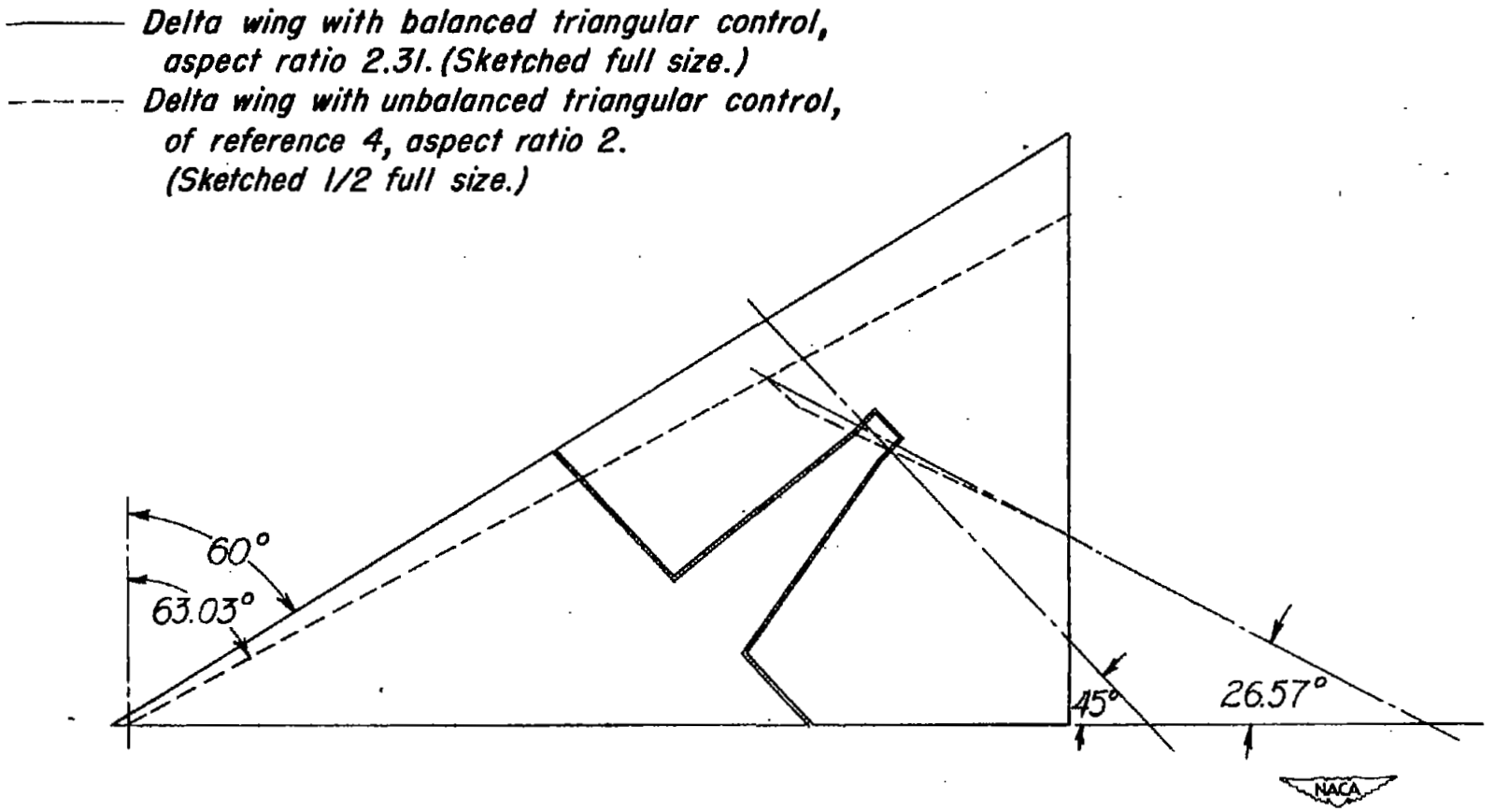

Figure 13.– Comparative sketches of general arrangements of the delta wing with balanced triangular control and delta wing with unbalanced triangular control of reference 4.

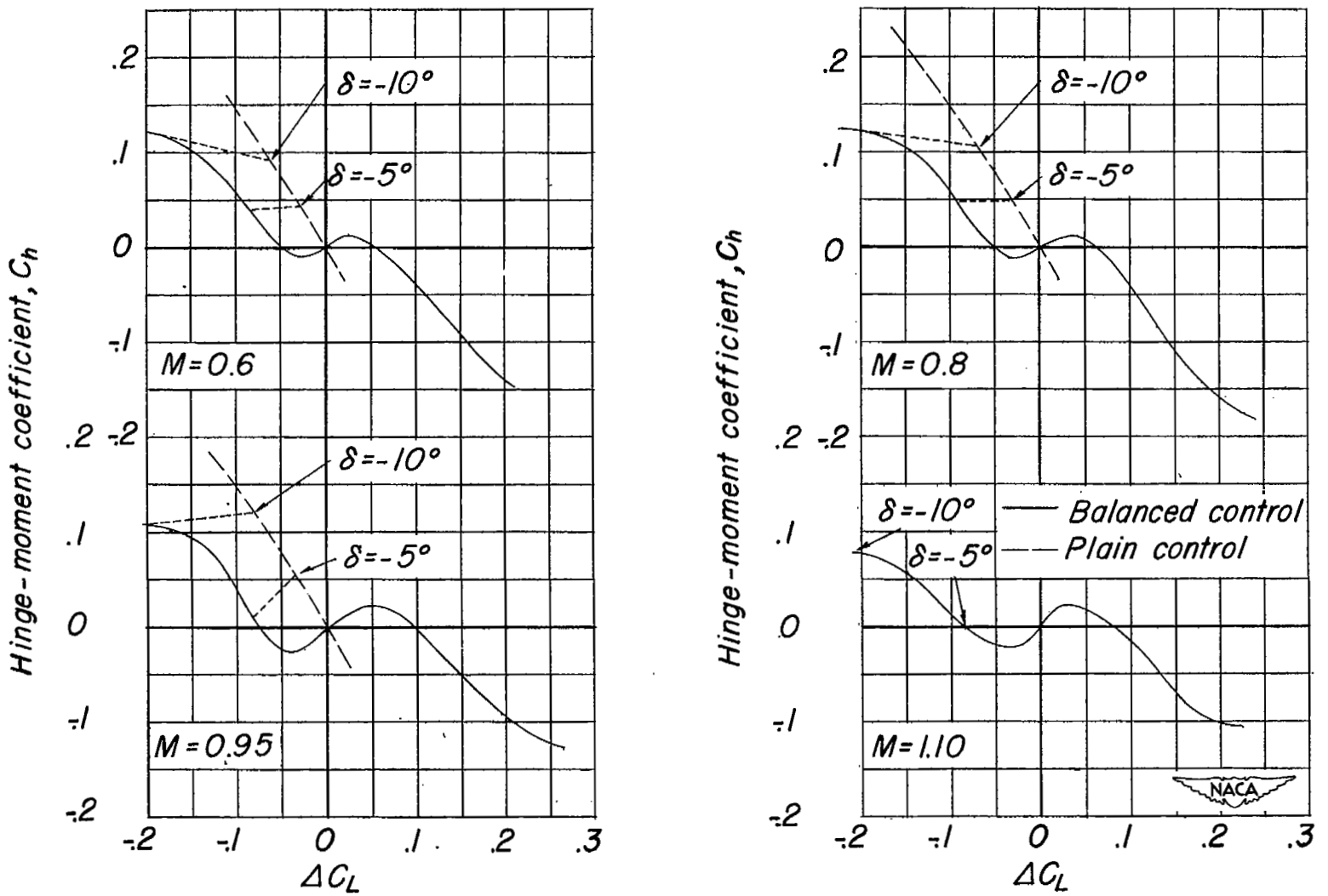

Figure 14.— The variation of hinge-moment coefficient with incremental lift coefficient for plain and triangular controls on a delta wing at $\alpha=0°$.

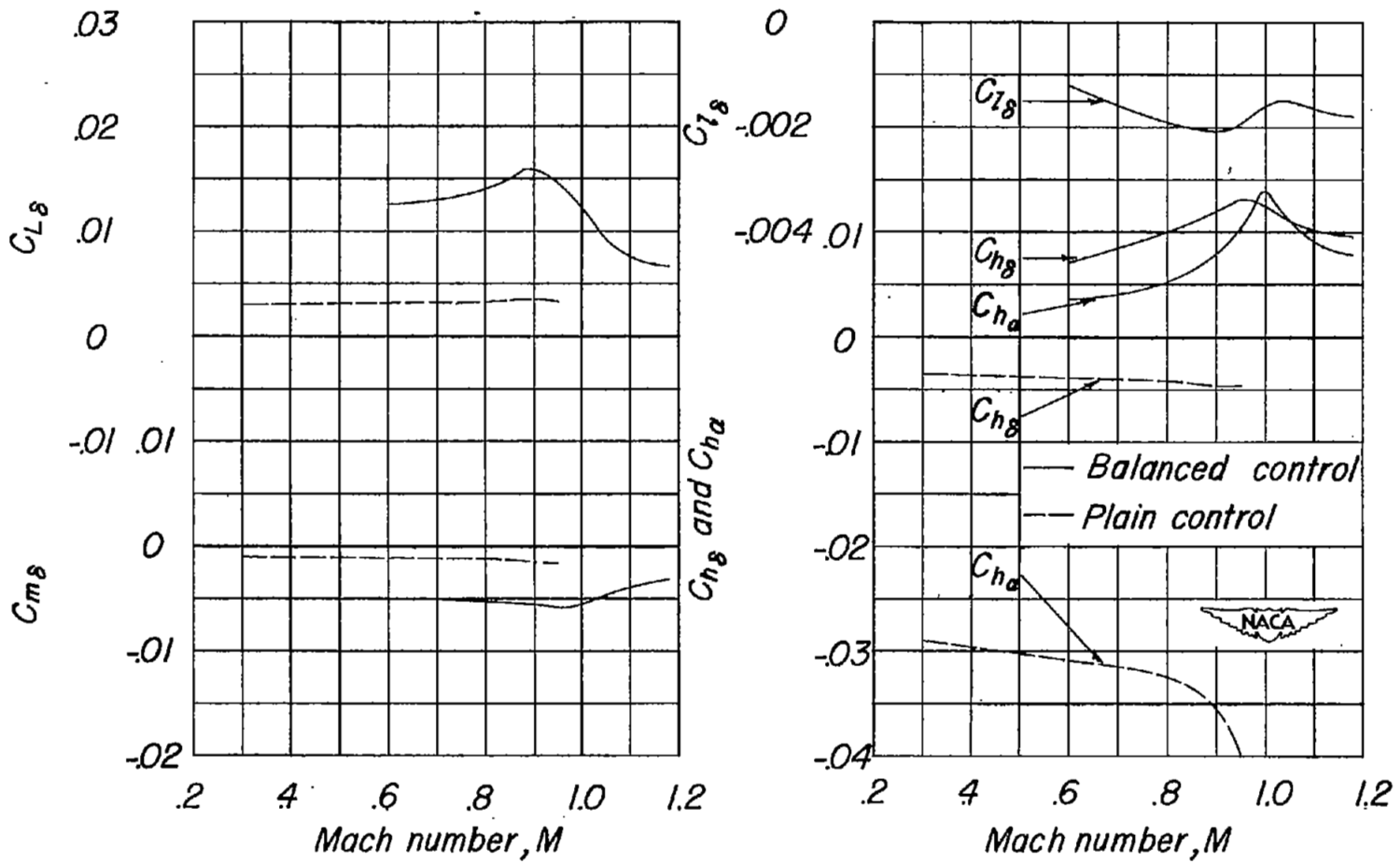

Figure 15.— The variation of the control parameters C_{L_δ}, C_{m_δ}, C_{l_δ}, C_{h_δ}, and C_{h_α} with Mach number for a triangular control with overhang balance and a plain triangular control on a delta wing. $\alpha = 0°$ and $\delta = 0°$